Published in final edited form as:
Traffic. 2010 January ; 11(1): 123–137. doi:10.1111/j.1600-0854.2009.00996.x.

Regulation of Insulin Secretion by Phosphatidylinositol-4,5-Bisphosphate

Alejandra Tomas[1], **Barbara Yermen**[1], **Romano Regazzi**[2], **Jeffrey E. Pessin**[3], and **Philippe A. Halban**[1]

[1]Department of Genetic Medicine and Development, University of Geneva Medical School, Geneva, Switzerland [2]Department of Cell Biology and Morphology, University of Lausanne, Lausanne, Switzerland [3]Departments of Medicine and Molecular Pharmacology, Albert Einstein College of Medicine, Bronx, New York, USA

Abstract

The role of PIP_2 in pancreatic beta cell function was examined here using the beta cell line MIN6B1. Blocking PIP_2 with PH-PLC-GFP or PIP5KIγ RNAi did not impact on glucose-stimulated secretion although susceptibility to apoptosis was increased. Over-expression of PIP5KIγ improved cell survival and inhibited secretion with accumulation of endocytic vacuoles containing F-actin, PIP_2, transferrin receptor, caveolin 1, Arf6 and the insulin granule membrane protein phogrin but not insulin. Expression of constitutively active Arf6 Q67L also resulted in vacuole formation and inhibition of secretion, which was reversed by PH-PLC-GFP co-expression. PIP_2 co-localized with gelsolin and F-actin, and gelsolin co-expression partially reversed the secretory defect of PIP5KIγ-over-expressing cells. RhoA/ROCK inhibition increased actin depolymerization and secretion, which was prevented by over-expressing PIP5KIγ, while blocking PIP_2 reduced constitutively active RhoA V14-induced F-actin polymerization. In conclusion, although PIP_2 plays a pro-survival role in MIN6B1 cells, excessive PIP_2 production due to PIP5KIγ over-expression inhibits secretion due to both a defective Arf6/PIP5KIγ-dependent endocytic recycling of secretory membrane and secretory membrane components such as phogrin and the RhoA/ROCK/PIP5KIγ-dependent perturbation of F-actin cytoskeleton remodeling.

Keywords

PIP_2; PIP5KIγ; insulin secretion; Arf6; endocytic recycling; RhoA/ROCK; F-actin

Introduction

Phosphatidylinositol-4,5-bisphosphate (PIP_2) is a minor cell membrane component that plays a critical role as a secondary messenger with levels rapidly modified after stimuli such as growth factors or binding to extracellular matrix (1;2). PIP_2 regulates a vast array of

Author for correspondence: Dr. Alejandra Tomas Department of Genetic Medicine and Development University of Geneva Medical School 1, rue Michel Servet 1211 Geneva 4 Switzerland Tel: +41 22 379 5527 Fax: +41 22 379 5528 Alejandra.TomasCatala@unige.ch.

cellular processes such as remodeling of the actin cytoskeleton (3), vesicle trafficking (4), and apoptosis (5;6).

Phosphatidylinositol 4-phospha t e 5-kinase I (PIP5KI) catalyses the major cellular route of PIP_2 synthesis. Three isoforms of PIP5KI (α, β and γ) have been cloned from the MIN6 pancreatic beta cell line (7;8). These are regulated by various factors including the small G protein family Rho (9) and Arf (10), which target each isoform to a specific cellular localization to produce PIP_2 (11). For example, PIP5KIγ is targeted to either focal adhesions (12) or adherent junctions (13) whereas PIP5KIα is targeted to the nucleus (14).

During actin remodeling, PIP_2 binds the N-terminal half of the actin severing protein gelsolin, inactivating it and causing its release from the severed actin filament thereby promoting actin polymerization (15). PIP_2 can also cause separation of actin monomers from actin monomer binding proteins, such as cofilin (16), thus enhancing actin nucleation leading to an overall increase in actin polymerization. As expected, over-expression of PIP5KI dramatically affects actin cytoskeleton dynamics by inducing stress fiber formation (17). On the contrary, reducing levels of PIP_2 blocks actin assembly and cell motility (18).

PIP_2 and PIP5KI also play a role in apoptosis. PIP_2 prevents apoptosis by inhibiting the activation of caspase 3 (19), possibly through the formation of a complex with gelsolin (20). On the other hand, cleavage inactivation of human PIP5KIα (homolog of murine PIP5Kβ) by caspase 3 has been shown to promote apoptosis (19). In addition, over-expression of human PIP5KIα or murine PIP5KIβ is thought to protect cells from apoptosis by either decreasing caspase 3 activation or promoting phosphorylation of ERK 1/2 (19;21).

PIP_2 and the Arf6-dependent regulation of PIP5KI are also implicated in the maintenance of large dense core vesicle (LDCV) exocytosis from neuroendocrine cells (22-24). PIP_2 has been shown to serve as a recruitment factor for proteins implicated in the priming of exocytic vesicles in a reconstituted assay (25). In pancreatic beta cells, where glucose regulates secretion of insulin through an intricate network of signaling pathways, both PIP_2 and the PIP5KI isoforms PIP5KIα and γ have been implicated in the maintenance of regulated secretion (26;27), although the precise mechanism of action has not been elucidated. Additionally, PIP_2 has been extensively implicated in clathrin-dependent endocytosis as a scaffold for many endocytic proteins (28), with the breakdown of PIP_2 by phosphatases required for the subsequent uncoating of endocytic vesicles (29). These observations have led to a proposed role for PIP_2 in the coordination of membrane fusion and fission with cytoskeletal assembly, providing a basis for membrane movement (4). PIP_2 has also been proposed to play a role in vesicle recapture during kiss-and-run exocytosis by the recruitment of dynamin and concerted action on actin (30).

In this study, we use the well-differentiated transformed mouse pancreatic beta cell line MIN6B1 to analyze the role of PIP5KIγ and PIP_2 in beta cell survival and insulin secretion, highlighting the importance of tightly controlled PIP_2 levels for the maintenance of beta cell function and identifying the main signaling pathways responsible for the regulation of the biological action of this key phospholipid on insulin secretion from pancreatic beta cells.

Results

The Pleckstrin Homology (PH) domain of phospholipase Cδ (PLCδ) specifically binds to PIP_2 and inhibits its interactions with other proteins (26;31) while allowing for its subcellular localization. As a first approach to investigate the role of PIP_2 in MIN6B1 cells we used a PH-PLC-GFP fusion protein in order to detect and specifically block PIP_2 biological action and PH-mutant-PLC-GFP (or PH-mut-PLC-GFP), a negative control unable to bind to PIP_2 as described by others. As expected, PH-PLCGFP localized to the plasma membrane of cells, where PIP_2 is primarily produced (1;22) (Figure 1A, top left panel), and co-localized with cortical F-actin (Figure 1A, bottom left panel), while PH-mut-PLCGFP was detected throughout the cytoplasm (Figure 1A, right panels). We used these constructs to analyze the impact of modulating availability of PIP_2 on the secretory response to glucose of MIN6B1 cells, using human growth hormone (hGH) as a surrogate marker for insulin secretion specifically from the population of transfected cells as previously described (32;33). MIN6B1 cells transfected with PH-PLC-GFP displayed no significant reduction of glucose-stimulated secretion (fold-stimulation) compared to cells transfected with PH-mut-PLC-GFP (Figure 1B). On the other hand, when we examined the susceptibility to cell death by apoptosis, there was a significant increase of TUNEL-positive cells after transfection with PHPLC-GFP compared to cells transfected with PH-mut-PLC-GFP or with the granule marker phogrin-GFP, used to monitor transfected cells as described in (34) (Figure 1C).

In order to confirm these results using an alternative strategy, we decreased PIP_2 levels by down-regulating PIP5KIγ using a previously described shRNA expression vector specific for this kinase (PIP5KI-RNAi) (26). Due to the low level of endogenous PIP5KIγ detected in MIN6B1 cells (see Figure 2A), these were co-transfected with a plasmid expressing PIP5KIγ fused to an HA tag (HA-PIP5KI) and either PIP5KI-RNAi or a control non-coding shRNA expression vector (Control-RNAi) in order to confirm the efficiency of the RNAi to knock-down PIP5KIγ, and levels of exogenously-expressed PIP5KIγ were analyzed by western blot with an antibody against the HA tag (Figure 1D). Transfection with PIP5KI-RNAi resulted in a 60% decrease on PIP5KIγ protein level compared to the control. In addition, we measured a 43±2.3% drop in the level of PIP5KIγ mRNA by quantitative PCR in cells expressing PIP5KI-RNAi vs. Control-RNAi (Figure 1E). This reduction was specific for the γ isoform of the kinase, as the relative mRNA levels of PIP5KI isoforms α and β were close to 1 ($\alpha=1\pm0.2$ and $\beta=0.92\pm0.04$, PIP5KI-RNAi vs. Control-RNAi). Next, we co-transfected MIN6B1 cells with either PIP5KI-RNAi or Control-RNAi and hGH, and measured glucose-stimulated secretion. As for cells expressing PH-PLC-GFP, there was no significant difference in the fold-stimulation of secretion (Figure 1F), indicating that the partial knockdown of PIP5KIγ does not have a negative impact on secretion. However, we found a significantly increased susceptibility to apoptosis in cells transfected with PIP5KI-RNAi compared to Control-RNAi, as shown by TUNEL and caspase 3 activation assays, with levels of apoptosis comparable to those obtained after gelsolin down-regulation with a gelsolin-specific shRNA expression vector (Gsn-RNAi) (Figure 1G).

In order to study the impact on secretion and apoptosis of increasing PIP_2 levels, MIN6B1 cells were transfected with HA tagged PIP5KIγ (HAPIP5KI), which resulted in a strong over-expression of the kinase in comparison to control cells (Figure 2A). We then analyzed

the secretory response to glucose in cells co-transfected with hGH and either HA-PIP5KI or a control empty vector. HA-PIP5KI-transfected cells presented a blunted secretion compared to the control resulting in the near complete loss of glucose responsiveness (Figure 2B). On the other hand, apoptosis (measured as a decrease in TUNEL-positivity) was decreased after transfection with HA-PIP5KI compared to the phogrin-GFP control (Figure 2C). Given the striking impairment in secretion caused by over-expression of HA-PIP5KI, we investigated the phenotype of these cells more closely. Confocal analysis of HAPIP5KI-transfected MIN6B1 cells revealed the formation of a large number of intracellular vacuoles (Figure 3A; see also Figures 3C and D). The membrane of these vacuoles contained HA-PIP5KI and PIP_2, and was coated with F-actin.

In order to characterize the importance of the F-actin coat for the formation of the vacuoles, we incubated cells transfected with HA-PIP5KI or a control empty vector in the presence of the F-actin depolymerising drug latrunculin B. The vacuoles were still present in HA-PIP5KI-trasfected cells after latrunculin B treatment, albeit with a modified morphology and disappearance of the actin coat surrounding them (Figure 3B, micrographs). As previously described by us (32), glucose-stimulated secretion of MIN6B1 cells was significantly increased after incubation with latrunculin B, and secretion was decreased in HA-PIP5KI-transfected cells as for Figure 2B (Figure 3B, bottom). When HA-PIP5KI-trasfected cells were treated with latrunculin B, glucose-stimulated secretion increased compared to non-treated HA-PIP5KI-trasfected cells, but the increase in secretion induced by the drug was lower than that exerted in control cells. Indeed, latrunculin B treatment resulted in 2±0.2-fold increase in the glucose response of control cells, while it only reached 1.4±0.2 in HA-PIP5KI-trasfected cells (Figure 3B, bottom).

To characterize the origin of the vacuoles in HAPIP5KI-trasfected cells, we performed a fluid uptake assay in which we incubated the cells with lysinefixable fluorescently-labeled dextran prior to fixation. Under these conditions, we could not detect any fluorescent signal present at the interior of the vacuoles in HA-PIP5KI-trasfected cells (Figure 3C, arrows), ruling out a macropinocytic origin for the vacuoles. We next performed a transferrin receptor (TfR) internalization assay in which we cotransfected MIN6B1 cells with HA-PIP5KI and a TfR expression vector and incubated them in the presence of fluorescent transferrin before fixation at 0°C or after 30 min incubation at 37°C. As expected, transferrin labeled the TfR at the cell surface at 0°C (Figure 3D, top, arrow) and was internalized after 30 min incubation at 37°C (Figure 3D, bottom). Transferrin was also incorporated in the membrane of the vacuoles (Figure 3D, bottom, arrows), indicating that the vacuolar membrane has, at least in part, a clathrin-dependent endocytic origin. We also detected the presence of the clathrin-independent endocytic marker caveolin 1 in the vacuolar membrane, suggesting that both clathrin-dependent and clathrin-independent endocytic pathways converged in PIP5KIγ over-expressing cells (Figure 3E).

Most of the above-mentioned experiments were based on manipulations of PIP5KIγ expression levels. In order to confirm that these were actually translated into differences in the level of intracellular PIP_2, we determined the amount of this phosphoinositide in lipid samples isolated from control MIN6B1 cells or from cells transfected with either PIP5KI-RNAi or HA-PIP5KI, using a specific PIP_2 ELISA test (Figure 4A). Cells displayed a 69%

reduction in the level of PIP_2 compared to the control after PIP5KIγ RNAi, while over-expression of PIP5KIγ resulted in a 17-fold increase in the amount of PIP_2. In an effort to rule out secondary effects of the variations in PIP_2 level on other phosphoinositide species, we attempted to determine the level of 2 phosphoinositides directly linked to PIP_2, namely PI4P and PIP_3, using specific protein-lipid overlay assays. For PI4P, we detected no differences in cellular levels after transfection with PIP5KI-RNAi or HA-PIP5KI compared to control cells (Figure 4B), while the level of PIP_3 was too low to allow for quantification in any of the conditions assayed (data not shown). In addition, and in order to rule out secondary effects of the manipulation of PIP_2 levels on the subcellular distribution of the other phosphoinositide lipids, we performed confocal microscopy analysis of cells co-transfected with either an empty vector, PIP5KI-RNAi or HAPIP5KI and a set of constructs expressing protein domains known to bind to specific phosphoinositides fused to fluorescent markers, widely used for intracellular localization of the different phosphoinositide species (28) (Figure 4C). As expected, specific detection of PIP_2 using the PH domain of PLCδ showed a reduction in fluorescence at the plasma membrane after transfection with PIP5KI-RNAi and an increase in fluorescence and accumulation of PIP_2-positive vacuoles in HAPIP5KI-expressing cells. However, neither PIP5KIRNAi nor HA-PIP5KI expression caused any differences compared to the control in the fluorescence intensity or intracellular localization of PI3P (using the tandem FYVE domain of Hrs, known to be localized primarily to endosomes), PI4P (with the PH domain of FAPP1, primarily localized to the Golgi apparatus) or PIP_3 (with the PH domain of Akt, partially localized to the plasma membrane).

Previous studies have reported that the activation of the small GTPase Arf6 also results in the accumulation of enlarged PIP_2-enriched vacuoles in the cell cytoplasm (10;35) and that it plays a role in Ca^{2+}-dependent exocytosis by regulating the activity of PIP5KI (23). We therefore examined the contribution of Arf6 to the formation of PIP5KIγ/ PIP_2-induced vacuoles and its impact on regulated secretion from MIN6B1 cells. First, we cotransfected MIN6B1 cells with a vector expressing Arf6 fused to a red fluorescent protein (Arf6 wt-DsRed Monomer) and PH-PLC-GFP for the detection of PIP_2. Confocal microscopy indicated that Arf6 and PIP_2 tightly co-localized at the plasma membrane level (Figure 5A), suggesting that Arf6 may induce the generation of PIP_2 by activation of PIP5KI at specific domains of the plasma membrane. Next, we analyzed the localization of wild type Arf6 (Arf6 wt), constitutively active Arf6 Q67L and dominant negative Arf6 T27N as GFP fusion proteins in cells over-expressing PIP5KIγ. Both Arf6 wt and Arf6 Q67L localized to the membrane of HA-PIP5KI-induced vacuoles, while this was much less apparent with dominant negative Arf6 T27N-GFP (Figure 5B). In addition, Arf6 Q67LDsRed-transfected cells accumulated F-actin-coated vacuoles similar to the ones found after transfection with HA-PIP5KI (Figure 5C). We also analyzed the secretory capacity of cells transfected with the different Arf6 constructs in the presence or absence of PH-PLC-GFP (to block PIP_2 protein binding interactions) (Figure 5D). Expression of Arf6 wt-HA or Arf6 Q67L-HA resulted in significant reductions in the fold-stimulation in secretion induced by glucose, this phenotype being more drastic for constitutively active Arf6 Q67L-HA and closely resembling that of PIP5KIγ over-expressing cells. Neither expression of the PIP_2 blocking plasmid PH-PLC-GFP nor dominant negative Arf6 T27N-HA had any effects on the fold-

increase in secretion of MIN6B1 cells. However, the secretory capacity of cells transfected with Arf6 Q67L-HA was partially restored by co-expression of PH-PLC-GFP (from 1.7±0.2 to 3.9±0.6 fold-stimulation), and, in parallel, the number of Arf6 Q67L-DsRed-transfected cells that presented vacuoles was greatly reduced after co-transfection with PH-PLC-GFP (from 39±3.6% to 7.45±2.4%) (Figure 5E). In addition, and as for transfection with HA-PIP5K, cells expressing Arf6 Q67L-GFP presented a decrease in apoptosis (measured as a decrease in TUNEL-positivity) when compared to phogrin-GFP-transfected control cells (Figure 5F). Taken together, these data suggest that constitutively active Arf6 Q67L is responsible for over-activation of PIP5KIγ leading to the accumulation of endocytic vacuoles and a secretion defect in MIN6B1 cells.

To investigate further the phenotype of PIP5KIγ over-expressing cells, we analyzed the subcellular localization of insulin granules in HA-PIP5KI-transfected MIN6B1 cells by co-transfection with a construct coding for phogrin fused to GFP, as phogrin is known to reside in the membrane of insulin granules (36). In addition to its granular localization, we surprisingly detected phogrin-GFP in the vacuoles of PIP5KIγ over-expressing cells (Figure 6A, top panels), while insulin was excluded from the vacuolar lumen (Figure 6A, bottom panels). Similar results were found in cells expressing constitutively active Arf6 Q67L-DsRed, in which phogrin-GFP was localized at the Arf6-induced vacuoles (Figure 6B, left) whereas neuropeptide Y (NPY) fused to a modified yellow fluorescence protein (NPY-Venus), used as a surrogate marker for LDCV secretion in living cells (37;38), was excluded from the vacuole interior (Figure 6B, right). These results suggest the existence of an Arf6/PIP5KIγ-dependent trafficking pathway implicated in the endocytic recycling of secretory granule membrane after exocytosis that is blocked at a post-internalization stage in cells transfected with HA-PIP5KI or Arf6 Q67L. Interestingly, we could observe some instances in cells cotransfected with phogrin-GFP and Arf6 wt-DsRed (which do not accumulate vacuoles) in which phogrin-GFP co-localized with the Arf6 wt-specific signal (Figure 6C top, arrows), but not insulin (Figure 6C, bottom), suggesting the existence of an Arf6-dependent endocytic recycling pathway through which phogrin would be transported on the recycling granular membrane following release of insulin.

We previously identified an important role for Ca^{2+}-dependent actin remodeling gelsolin in the regulation of insulin secretion (32). Given the well established role of PIP_2 in gelsolin inhibition (39), we investigated whether the secretory phenotype observed after over-expression of PIP5KIγ was, at least in part, dependent on defects in actin cytoskeleton remodeling due to impaired gelsolin function. First, we analyzed the localization of PIP_2, F-actin and gelsolin in MIN6B1 cells transfected with PH-PLC-GFP. The PIP_2-specific signal co-localized with F-actin at the plasma membrane (Figure 7A, top panels) and with cytoplasmic gelsolin (Figure 7A, bottom panels). We next analyzed the level of secretion of MIN6B1 cells co-transfected with hGH and a gelsolin shRNA-expressing vector (Gsn-RNAi) in conjunction with HA-PIP5KI (Figure 7B, top graph). As we previously reported (32), gelsolin knockdown resulted in a significant decrease of glucose-stimulated secretion compared to the control. In addition, co-expression of both Gsn-RNAi and HA-PIP5KI significantly reduced glucose-stimulated secretion compared to cells transfected with Gsn-RNAi alone, resulting in the near complete loss of secretory response to glucose. We also analyzed the level of secretion of cells over-expressing both PIP5KIγ and gelsolin by co-

expression of HA-PIP5KI and a vector coding for gelsolin fused to an HA tag (HA-Gsn) (Figure 7B, bottom graph). As expected, HA-PIP5KI-transfected cells displayed markedly reduced glucose-stimulated secretion compared to the control. Over-expression of gelsolin partially prevented the decrease in glucose-stimulated secretion of HAPIP5KI-transfected cells, suggesting that PIP_2 inhibition of gelsolin contributes to the secretory loss in cells over-expressing PIP5KIγ.

As the over-activation of PIP5KIγ by Arf6 seems to be responsible for a defect in the endocytic recycling of secretory membrane without any obvious impact on the actin cytoskeleton, we wished to identify other signaling pathways that could be responsible for the over-activation of PIP5KIγ linked to impaired actin cytoskeleton remodeling. The RhoA/Rho Kinase (ROCK) pathway is well known to play important roles in act in cytoskeleton remodeling (40), can act via activation of PIP5KI and PIP_2 production (9;41), and as we have recently shown (42), has an impact on F-actin remodeling and insulin secretion in primary beta cells. As for Figures 2, 3 and 7, transfection with HA-PIP5KI resulted in a significant reduction of glucose-stimulated secretion while, in agreement with our previous results in primary beta cells (42), pre- incubation with the ROCK inhibitors Y-27632 or H-1152 resulted in a significant increase of secretion compared to control cells (Figure 8A). This increase was no longer present in cells with both ROCK inhibition and PIP5KIγ over-expression. Inhibition of the RhoA/ROCK pathway had no impact on the formation of vacuoles in PIP5KIγ over-expressing cells, as HA-PIP5KI-transfected cells still accumulated vacuoles after treatment with Y-27632 or H-1152 (Figure 8B). On the other hand, and as for primary beta cells, ROCK inhibition resulted in increased cortical F-actin depolymerization with MIN6B1 cells exhibiting shorter actin fibers at the sub-plasmalemmal level than untreated control cells (Figure 8C).

We next investigated the effects of the over-activation of RhoA on actin cytoskeleton remodeling in MIN6B1 cells using the plasmid RhoA V14-myc, which codes for a constitutively active mutant of RhoA fused to a myc tag and has previously been shown to inhibit regulated secretion in PC12 cells (43). Cells transfected with RhoA V14-myc presented an abnormally condensed cortical F-actin cytoskeleton compared to untransfected cells from the same dish, with presence of thick actin fibers that did not remodel in the presence of glucose (Figure 9A, red arrows). In contrast to Arf6 Q67L, RhoA V14-myc-transfected cells did not accumulate endocytic vacuoles (data not shown). Conversely, transfection with Arf6 Q67L-HA did not have any effect on cortical actin while, as already mentioned above (Figure 5C), it led to the formation of cytoplasmic vacuoles (Figure 9B). In order to determine if PIP_2 was responsible for the defect in actin cytoskeleton remodeling in cells expressing RhoA V14, we co-transfected MIN6B1 cells with RhoA V14-myc and PH-PLC-GFP in order to block PIP_2 (Figure 9C). These cells presented a cortical actin cytoskeleton that was less condensed than that of cells transfected with RhoA V14-myc alone, and was similar to that of untransfected cells from the same dish (Figure 9C, red arrows; compare to Figure 9A). Taken together, these experiments demonstrate that over-activation of PIP5KIγ by RhoA/ROCK results in cortical actin cytoskeleton remodeling defects that impact negatively on regulated secretion. This appears to be separate from the impact of over-activation of PIP5KIγ by Arf6, which results in impaired secretion due to a

defect on endocytic recycling of secretory membrane and subsequent trapping of granular membrane components in abnormal endocytic vacuoles.

Discussion

PIP5KI was first linked to exocytosis in an early screening of cytoplasmic factors required for ATP-dependent priming in PC12 cells (44). A role for PIP_2 was inferred as PIP5KI is known to use ATP to synthesize this phospholipid. Subsequent studies reported that over-expression of the pleckstrin homology domain of phospholipase Cδ, which specifically binds to PIP_2 thereby preventing its biological function, reduced Ca^{2+}-dependent exocytosis in chromaffin cells (22) and glucose-stimulated secretion in the pancreatic beta cell line INS1E (26). Secretion defects identified in chromaffin cells that had nearly completely lost PIP_2 by over-expressing the PIP_2-phosphatase synaptojanin 1 (24) or in PIP5KIγ knockout mice (45) led to the conclusion that PIP_2 stimulates exocytosis by increasing the size of the readily releasable pool of vesicles due to increased priming. Recent reports have however pointed out a more complicated role for this phospholipid in regulated LDCV exocytosis. As well as a positive role in the recruitment of priming factors, PIP_2 was shown to inhibit SNARE-dependent liposome fusion. This inhibition was proposed to be based on its intrinsic positive membrane curvature-promoting properties as an inverted cone-shaped lipid (25). In addition, PIP5KI activity and PIP_2 levels were shown not to be modulated by stimulation with secretagogues in PC12 cells (46).

We could not detect any deleterious effect on the secretory capacity of MIN6B1 cells of reducing the level of active PIP_2 by expression of PH-PLC-GFP or by partial knockdown of PIP5KIγ. We interpret these results as the consequence of a dual (positive and negative) role of PIP_2 in insulin granule exocytosis. Any secretion phenotypes would therefore require severe inhibition of PIP_2 in order to be detected, as we believe that in MIN6B1 cells with a partial decrease in PIP_2 levels, reduced granule priming would be compensated by increased membrane fusion.

Regardless of these considerations, the present study shows for the first time a clear role of PIP_2 as a pro-survival factor in pancreatic beta cells. Both expression of PH-PLC-GFP and PIP5KIγ RNAi resulted in increased susceptibility to apoptosis, a phenotype that was reversed by over-expression of PIP5KIγ with the HA-PIP5KI construct. PIP_2 has been shown to have anti-apoptotic properties due to its capacity to inhibit caspase 3 activity through the formation of a PIP_2-gelsolin-caspase complex (19;20). We have previously identified gelsolin as an anti-apoptotic protein that blocks activation of caspase 3 in MIN6B1 and primary beta cells (34). Here we show that PIP5KIγ RNAi results in increased levels of caspase 3 activation similar to those found after gelsolin RNAi. We therefore hypothesize that PIP_2 plays a role as a pro-survival factor in conjunction with gelsolin by caspase 3 inhibition in pancreatic beta cells. Further experiments that fall outside of the scope of this study will be required to confirm this hypothesis.

Aside from a reduction in apoptosis, over-expression of PIP5KIγ resulted in the near complete abolishment of the secretory response to glucose in MIN6B1 cells. This effect is different to that found in other neuroendocrine cell types, such as chromaffin cells (24) or

the PC12 cell line (47), where exogenous expression of murine PIP5KIγ or β, respectively, potentiated secretion. Intracellular application of PIP_2 has been shown to stimulate exocytosis in pancreatic beta cells (48) and in the beta cell line INS1E (26). However, the effect of PIP5KIγ over-expression in beta cells has not been investigated before. In this context, it is worth noting that in the present study transfection with HAPIP5KI resulted in a vast increase in the amount of PIP5KIγ (taking into account that only ~15% of cells were transfected and the mixed population of transfected and untransfected cells presented a 6-fold increase as observed by Western blot) and in a 17-fold increase in the level of PIP_2 compared to untransfected cells. This might explain the appearance of a phenotype that would not be apparent in a less extreme environment or in the special situation of patch-clamped (48) or streptolysin-O permeabilized cells (26). Under our experimental conditions, transfection with HAPIP5KI led to the accumulation of PIP_2-enriched cytoplasmic vacuoles that had an endocytic origin. Whether or not similar vacuoles appear in beta cells following direct application of PIP_2 was not documented in the earlier studies (26;48). Similar vacuoles have been observed in the past after over-expression of mouse PIP5KIβ in 293T cells (49) and mouse PIP5KIβ or γ in 3T3L1 adipocytes (50), as well as in nerve terminals of mice lacking the PIP_2-phosphatase synaptojanin (29). In agreement with (50), PIP5KIγ-induced vacuoles resulted from convergence of both clathrin-dependent and clathrin-independent endocytosis and were coated with actin. Although disruption of the F-actin coat increased glucose-stimulated secretion in PIP5KIγ over-expressing cells, the vacuoles were still present (albeit with a changed morphology) and the increase in the fold-stimulation of secretion elicited by latrunculin B was proportionally lower to that in control cells. This indicates that disruption of the F-actin coat is not sufficient to reverse the phenotype observed in PIP5KIγ over-expressing cells, which must harbor a defect in the trafficking of endocytic membrane and possibly a reduced capacity in actin cytoskeleton remodeling that would explain the lower efficiency of latrunculin B in potentiating glucose-stimulated secretion secretion.

Given that PIP_2 plays an important role in the assembly of endocytic vesicles via the recruitment of essential vesicle coating factors, and that subsequent PIP_2 degradation by phosphatases is required for the uncoating of these vesicles (29;51) we hypothesize that the over-production of PIP_2 in PIP5KIγ over-expressing beta cells may lead to a defect in the uncoating of endocytic vesicles that results in accumulation of abnormal vacuoles due to a halt in the endocytic trafficking pathway.

In this regard, we have investigated the role of Arf6 as a candidate GTPase responsible for the activation of PIP5KIγ specifically to function in the endocytic pathway of MIN6B1 cells. Arf6-GTP (but not Arf6-GDP) has been found to interact with and activate PIP5KIγ in order to facilitate the assembly of clathrin-coated pits required for the endocytic recycling of synaptic vesicle membrane (52). We could observe extensive co-localization of Arf6 and PIP_2 in discrete loci at the plasma membrane of MIN6B1 cells. In addition, both Arf6 wt and constitutively active Arf6 Q67L localized to the membrane of PIP5KIγ-induced vacuoles, this being much less evident for dominant negative GDP-bound Arf6 T27N. Arf6 Q67L has been shown previously to induce the formation of PIP_2-positive actin-coated endocytic vacuoles that mimic those found after PIP5KI over-expression (10;35). In agreement with these reports, Arf6 Q67L expression in MIN6B1 cells resulted in the

accumulation of F-actin-coated vacuoles. More importantly, this was accompanied by a reduction in the secretory fold-stimulation similar to that found after PIP5KIγ over-expression, with partial restoration of secretion together with a significant reduction in the number of vacuole-containing Arf6 Q67L-expressing cells by co-expression of the PIP_2-blocking construct PHPLC-GFP. Conversely, and contrary to a previous report (53), expression of the dominant negative mutant Arf6 T27N did not have any effect on glucose-stimulated secretion in MIN6B1 cells.

Arf6 Q67L expression has previously been reported to cause inhibition of Ca^{2+}-dependent exocytosis and accumulation of PIP5KI and PIP_2 on endosomal membranes in PC12 cells (23). In the cited study exocytosis was restored by co-over-expression of PIP5KIγ, leading the authors to conclude that the secretory defect was due to the abnormal trapping of PIP5KI by Arf6 Q67L on endosomes and the subsequent depletion of PIP_2 from the plasma membrane. Our results show a very different picture. In fact, co-over-expression of PIP5KIγ and Arf6 Q67L in MIN6B1 cells did not lead to any improvement in glucose stimulated secretion (data not shown), a result somewhat expected by us due to the highly impaired secretion observed in PIP5KIγ-expressing MIN6B1 cells. We therefore conclude that the inhibition of secretion observed in MIN6B1 cells is not due to trapping of PIP5KIγ on endosomes but rather to over-production of PIP_2 by either over-expression of PIP5KIγ or over-activation of PIP5KIγ by Arf6 Q67L.

In this study we have also identified a link between an endocytic trafficking defect and the secretion impairment observed in PIP5KIγ- or Arf6 Q67L-expressing MIN6B1 cells, namely the trapping of secretory membrane proteins such as phogrin (but not secretory granule contents, i.e. insulin) in endocytic vacuoles. Endocytic recycling of secretory membrane and secretory membrane components following exocytosis is considered to be an important step in the regulation of glucose-stimulated insulin secretion (30;54-57), perhaps involving a dynamin-1-dependent recapture process following kiss-and-run exocytosis (30), however the exact trafficking pathways downstream of this recapture have remained obscure. Here we show these to involve an Arf6/PIP5KIγ-dependent pathway and highlight its importance for the correct regulation of insulin secretion in beta cells.

In addition to its role in membrane trafficking, PIP_2 can affect actin cytoskeleton dynamics via the regulation of key factors involved in F-actin remodeling (for a review see (58)). We have previously shown that the Ca^{2+}- and PIP_2-dependent actin severing protein gelsolin plays an important role in regulated secretion from MIN6 cells, likely through F-actin remodeling (32). Gelsolin activity and F-actin remodeling following a glucose-dependent rise in intracellular Ca^{2+} are thus required to maintain optimal levels of insulin secretion. Here we show that the defect in secretion due to the overproduction of PIP_2 is further accentuated by down-regulating gelsolin and on the other hand is partially rescued by gelsolin over-expression. Given this and the tight co-localization of PIP_2, gelsolin and F-actin at the plasma membrane of MIN6B1 cells, we conclude that increased inhibition of gelsolin by PIP_2 is partially responsible for the negative impact of excess PIP_2 on insulin secretion.

We have recently published a study showing a positive effect of inhibition of RhoA/ROCK signaling pathway on insulin secretion linked to increased F-actin remodeling (42). Based on this and on previous studies revealing an intimate crosstalk between this GTPase, PIP_2 and actin we have analyzed the role of this pathway in the activation of PIP5KIγ to function in F-actin dynamics. We now establish that MIN6B1 cells display an analogous response to rat primary beta cells after short-term inhibition of ROCK, resulting in increased glucose stimulated secretion and cortical F-actin depolymerization. Inhibition of ROCK in conjunction with over-expression of PIP5KIγ leads to the loss of the positive effect of ROCK inhibition on secretion but has no effect on the accumulation of vacuoles driven by excessive PIP_2 production. Conversely, constitutive activation of RhoA, known to have a negative impact on regulated secretion (43), results in increased F-actin polymerization but does not lead to the accumulation of endocytic vacuoles as for constitutively active Arf6. In addition, the defect on F-actin remodeling exhibited by constitutively active RhoA-expressing cells can be (partially) rescued by blockage of PIP_2 with PH-PLC-GFP. All of these data suggest that RhoA/ROCK signaling pathway activity contributes to the over-activation of PIP5KIγ (and consequently over-production of PIP_2) resulting in a negative impact in the capacity of cells to remodel their actin cytoskeleton in response to glucose, most probably due to an excessive inhibition of actin remodeling proteins such as gelsolin by PIP_2.

In conclusion, we show for the first time that PIP_2 plays a pro-survival role in MIN6B1 cells. However, protection against apoptosis granted by excess PIP_2 due to PIP5KIγ over-expression is associated with a very negative impact on regulated secretion. The inhibition of secretion results from a halt in the Arf6/PIP5KIγ-dependent endocytic recycling of secretory membrane and secretory membrane components such as phogrin, and by the perturbation of F-actin remodeling due to the RhoA/ROCK/PIP5KIγ-dependent inhibition of actin remodeling proteins such as gelsolin by PIP_2.

These results highlight the importance of maintaining tightly controlled PIP_2 levels for the regulation of beta cell function under physiological conditions, as this phospholipid is implicated in beta cell survival and in the control of two important processes for insulin secretion (in addition to its reported effects on granule priming and fusion), namely actin cytoskeleton remodeling and the endocytic recycling of secretory membrane.

Materials and Methods

Reagents and Antibodies

Latrunculin B and the ROCK inhibitors H-1152 and Y-27632 were purchased from Calbiochem (San Diego, CA) and used at 10 μM, 10 μM and 50 μM, respectively. DNA was stained with Draq5™ from Biostatus Ltd. (UK) and F-actin was visualized using phalloidin-AlexaFluor 546 and phalloidin-AlexaFluor 647, from Invitrogen (Carlsbad, CA). The PH-FAPPYFP construct was obtained from The Division of Signal Transduction Therapy, University of Dundee, UK. Primary antibodies were mouse anti-HA tag from Roche (Basel, Switzerland); rabbit anti-cleaved caspase-3 and mouse anti-myc tag from Cell Signaling Technology (Danvers, MA); mouse anti-PIP5Kγ and rabbit anti-caveolin 1 from BD Biosciences (Franklin Lakes, NJ); rabbit anti-gelsolin (a gift from Dr. C. Chaponnier,

University of Geneva Medical School, Switzerland); mouse anti-actin from Chemicon International (Temecula, CA); and guinea pig anti-insulin (from Dr. D. Bosco, University of Geneva Medical School, Switzerland). Secondary antibodies were sheep anti-mouse HRP and donkey anti-rabbit HRP from Amersham Biosciences (Uppsala, Sweden); and goat anti-mouse AlexaFluor 488, donkey anti-rabbit AlexaFluor 555, donkey anti-mouse AlexaFluor 555, and goat anti-guinea pig AlexaFluor 488 from Invitrogen.

MIN6B1 Cell Culture Conditions

MIN6B1 cells were cultured in DMEM supplemented with 15% FCS, 25 mM glucose, 71 μM 2-mercaptoethanol, 2 mM glutamine, 100 U/ml penicillin and 100 mg/l streptomycin at 37°C in an atmosphere of humidified air (95%) and CO_2 (5%) as previously described (59). In general, cells up to passage 25 were sub-cultured into 35 mm wells to ~80% confluency before the experiments. For confocal microscopy cells were plated onto 35-mm glass bottom micro-well dishes (MatTek, Ashland, MA, USA) coated with extracellular matrix from 804G rat bladder carcinoma cells to favor cell attachment (60).

Transient Transfections

Cells were transfected using Lipofectamine™ 2000 (Invitrogen) according to the manufacturer's instructions. Transfected cells were incubated for 48 h to allow for construct expression or 72 h for RNAi.

Growth Hormone Secretion Assays

To study secretion from transfected cells only, cells were co-transfected with the hGH-expressing vector pcDNA3-hGH and the vector of interest (1:3 DNA ratio). After 48-72 h cells were analyzed for hGH release, which was used as a surrogate marker for insulin secretion only from co-transfected cells (61). To this end, co-transfected cells were washed twice in a modified Krebs–Ringer bicarbonate HEPES buffer [KRBH: 125 mM NaCl, 4.74 mM KCl, 1 mM $CaCl_2$, 1.2 mM KH_2PO_4, 1.2 mM $MgSO_4$, 5mM $NaHCO_3$, 25 mM HEPES (pH 7.4) and 0.1% BSA] with 2.8 mM glucose and pre-incubated in this same buffer for 2 h at 37°C. Cells were then incubated for 1 h at 37°C in KRBH with 2.8 mM glucose (basal condition), followed by 1 h incubation with KRBH + 16.7 mM glucose (stimulated condition). Cells were extracted with acid-ethanol, and the amount of growth hormone in the incubation buffers and cell extracts was measured with the hGH ELISA kit from Roche Diagnostics (Basel, Switzerland), following the manufacturer's instructions. Growth hormone secretion is expressed as a percentage of the total growth hormone content, which is the sum of growth hormone contained in the buffers and cell extracts.

TUNEL and Caspase-3 Activation Assays

Transfected MIN6B1 cells were incubated for 24 h in standard conditions (25 mM glucose; 15% FCS) before inducing apoptosis for 48 h in deprived conditions (5 mM glucose and 1% FCS). Cells were washed in PBS and fixed with 4% paraformaldehyde. After permeabilization with 0.5% Triton X-100 a TUNEL assay, which detects DNA strand breaks formed during apoptosis (62), was performed using the In Situ Cell Death Detection Kit (Roche Diagnostics) according to the manufacturer's instructions.

Nuclei were stained with 1 μg/ml Hoechst 33342 and activation by cleavage of caspase-3 was determined by immunofluorescence using an antibody specific for the active cleaved form of the protein.

Transferrin Receptor Endocytosis Assay

Clathrin-dependent endocytosis was analyzed by TfR internalization assay as described previously (50). Briefly, MIN6B1 cells were co-transfected with a plasmid encoding human TfR and with HAPIP5KI. After 48 h, cells were washed and pre-incubated for 1 h in serum-free DMEM, then chilled on ice and incubated for 30 min with 100 μg/ml AlexaFluor 555-human transferrin (Invitrogen) to label the surface TfR. After a further 3 washes in ice-cold serum-free DMEM, 1 dish of cells was fixed in 2 % paraformaldehyde while another dish was incubated at 37°C for 30 min to allow for transferrin-TfR internalization before fixation. Both dishes were subsequently processed by immmunofluorescence and confocal microscopy.

Fluid Phase Uptake Assay

Pinocytosis was assayed by a fluid phase uptake protocol as follows: MIN6B1 cells previously transfected with HA-PIP5KI were washed in serum-free DMEM and incubated at 37°C for 30 min in 1 mg/ml lysine-fixable Texas Red-dextran 3000 MW (Invitrogen). Cells were then chilled on ice, washed 3 times with ice-cold serum-free DMEM, fixed and processed for immunofluorescence and confocal microscopy.

Immunofluorescence and Confocal Microscopy

Cells were washed in PBS, fixed/permeabilized on i c e f o r 3 0 min in 2% paraformaldehyde supplemented with 0.1% Triton X-100 in PBS, washed again in PBS and blocked for 15 min with 1% BSA. Fixed cells were incubated with primary followed by secondary antibody in 1% BSA for 1 h. Cells were observed under a Zeiss LSM 510 inverted confocal microscope using a 63× oil immersion lens. Images were acquired and processed using the Lsm510 software (Carl Zeiss AG, Germany).

SDS-PAGE and Western Blotting

Cells were washed in PBS and solubilized in lysis buffer (20 mM Tris, pH 7.5, 1 mM EDTA, 1 mM EGTA, 150 mM NaCl, 1% NP-40) + Complete Mini protease inhibitor cocktail (Roche, Basel, Switzerland). Lysates were pre-cleared at 16,000 g for 5 min at 4°C, and total protein levels were quantified using the detergent-compatible protein assay kit (BioRad, Hercules, CA). Protein samples were re-suspended in SDS-PAGE sample buffer (62 mM Tris-HCl, pH 6.8, 2% SDS, 5% glycerol, and 1% 2-mercaptoethanol), boiled for 5 min and resolved on a 10% SDS-polyacrylamide discontinuous mini-gel. Proteins were then electroblotted for 45 min onto a Protran nitrocellulose Transfer Membrane (S c h l e i c h e r & S c h u e l l G m b H , G e r m a n y) . Membranes were treated with blocking solution (5% skimmed milk in TBS + 0.1% Tween 20) for 1 h at RT, and incubated for 16 h at 4°C with primary antibody in blocking solution. Following three TBSTween washes, membranes were incubated with secondary antibody for 90 min in blocking solution. After three more washes, blots were incubated with the ECL Plus Western blotting detection system

(Amersham Biosciences) and exposed onto BioMax MR Films (Kodak, Rochester, NY). The films were developed in a Kodak M35 X-OMAT Processor and the resulting bands were scanned and analyzed with Multi Gauge V3.0 (Fujifilm Life Science, Tokyo, Japan).

Quantitative Real-Time PCR

Cells were co-transfected with pEGFP and either pSUPER-Control RNAi or pSUPER-PIP5KI RNAi (1:3 DNA ratio). After 72 h, GFP-positive cells were isolated by FACS and total RNA was extracted with the RNeasy Mini kit (Qiagen, Germany) following the manufacturer's instructions, and used for cDNA synthesis with Superscript II (Invitrogen) and Oligo dT primer (Promega, Madison, USA). Specific primers for each of the mouse PIP5KI isoforms were designed using the Primer Express software, and real-time PCR was performed using the qPCR core kit for SYBR Green I (Eurogentec, Belgium) in the iCycler iQ System (BioRad). Relative mRNA expression was normalized with the housekeeping gene cyclophilin.

Cell Extraction of Phosphoinositides

Transfected cells were trypsinised, counted and pelleted before adding 0.5% ice cold TCA (1 ml/10^6 cells). After 5 min incubation on ice, samples were centrifuged at 1500 rpm for 5 min and pellets were washed in 5% TCA + 1 mM EDTA and centrifuged. The neutral lipids were extracted by vortexing 3 times over 10 min at RT in MeOH:$CHCl_3$ (2:1) followed by centrifugation. The acidic lipids were also extracted in the same manner by vortexing 4 times over 15 min at RT in MeOH:$CHCl_3$:HCl (80:40:1) at RT followed by centrifugation. A phase split was performed on the supernatant by adding $CHCl_3$ (0.15 ml/10^6 cells) + 0.1 M HCl (0.27 ml/10^6 cells), vortexing and spinning down at 1500 rpm for 5 min. The lower organic phase was collected and dried in a vacuum dryer. Dried lipids were stored at −20°C until processed.

Analysis of Phosphoinositide Levels

Phosphoinositide samples were reconstituted, vortexed and sonicated in the appropriate solution immediately before use. The amount of PIP_2 in the purified reconstituted samples was measured by ELISA using the PI(4,5)P_2 Mass ELISA Kit (Echelon Biosciences, Salt Lake City, USA) according to the supplier's instructions. For PI4P and PIP_3 quantifications, the lipid samples were reconstituted in $CHCl_3$:MeOH:H_2O (1:2:0.8) and spotted onto membranes from the PI4P or the PIP_3 Mass Strip Kits (Echelon Biosciences).

Statistics

Data are presented as mean ± SEM for n independent experiments. Statistical significance of differences between groups was evaluated by Student's unpaired two-tailed t-test with $p<0.05$ considered significant.

Acknowledgments

We thank Stéphane Dupuis and Katharina Rickenbach for expert technical assistance, Prof. J. Donaldson (NHLBI, NIH, USA) for the Arf6 vectors, Prof. T. Balla (NICHD, NIH, USA) for the PH-Akt-GFP plasmid and Prof. H. Stenmark (Institute for Cancer Research, Oslo, Norway) for the PH-2xFYVE-GFP plasmid. This work was

supported by grant numbers 310000-113967/1 (PAH) and 3100A0-113421 (RR) from the Swiss National Science Foundation and NIH grant number 5-R01-DK063332 (JP and PAH).

References

1. Doughman RL, Firestone AJ, Anderson RA. Phosphatidylinositol phosphate kinases put PI4,5P(2) in its place. J Membr Biol. 2003; 194:77–89. [PubMed: 14502432]
2. Takenawa T, Itoh T. Phosphoinositides, key molecules for regulation of actin cytoskeletal organization and membrane traffic from the plasma membrane. Biochim Biophys Acta. 2001; 1533:190–206. [PubMed: 11731330]
3. Yin HL, Janmey PA. Phosphoinositide regulation of the actin cytoskeleton. Annu Rev Physiol. 2003; 65:761–789. [PubMed: 12471164]
4. Martin TF. PI(4,5)P(2) regulation of surface membrane traffic. Curr Opin Cell Biol. 2001; 13:493–499. [PubMed: 11454457]
5. Bunce MW, Gonzales ML, Anderson RA. Stress-ING out: phosphoinositides mediate the cellular stress response. Sci STKE. 2006; 2006:e46.
6. Oude Weernink PA, Schmidt M, Jakobs KH. Regulation and cellular roles of phosphoinositide 5-kinases. Eur J Pharmacol. 2004; 500:87–99. [PubMed: 15464023]
7. Ishihara H, Shibasaki Y, Kizuki N, Katagiri H, Yazaki Y, Asano T, Oka Y. Cloning of cDNAs encoding two isoforms of 68-kDa type I phosphatidylinositol-4-phosphate 5-kinase. J Biol Chem. 1996; 271:23611–23614. [PubMed: 8798574]
8. Ishihara H, Shibasaki Y, Kizuki N, Wada T, Yazaki Y, Asano T, Oka Y. Type I phosphatidylinositol-4-phosphate 5-kinases. Cloning of the third isoform and deletion/substitution analysis of members of this novel lipid kinase family. J Biol Chem. 1998; 273:8741–8748. [PubMed: 9535851]
9. Weernink PA, Meletiadis K, Hommeltenberg S, Hinz M, Ishihara H, Schmidt M, Jakobs KH. Activation of type I phosphatidylinositol 4-phosphate 5-kinase isoforms by the Rho GTPases, RhoA, Rac1, and Cdc42. J Biol Chem. 2004; 279:7840–7849. [PubMed: 14681219]
10. Brown FD, Rozelle AL, Yin HL, Balla T, Donaldson JG. Phosphatidylinositol 4,5-bisphosphate and Arf6-regulated membrane traffic. J Cell Biol. 2001; 154:1007–1017. [PubMed: 11535619]
11. Santarius M, Lee CH, Anderson RA. Supervised membrane swimming: small G-protein lifeguards regulate PIPK signalling and monitor intracellular PtdIns(4,5)P2 pools. Biochem J. 2006; 398:1–13. [PubMed: 16856876]
12. Ling K, Doughman RL, Firestone AJ, Bunce MW, Anderson RA. Type I gamma phosphatidylinositol phosphate kinase targets and regulates focal adhesions. Nature. 2002; 420:89–93. [PubMed: 12422220]
13. Akiyama C, Shinozaki-Narikawa N, Kitazawa T, Hamakubo T, Kodama T, Shibasaki Y. Phosphatidylinositol-4-phosphate 5-kinase gamma is associated with cell-cell junction in A431 epithelial cells. Cell Biol Int. 2005; 29:514–520. [PubMed: 15994099]
14. Boronenkov IV, Loijens JC, Umeda M, Anderson RA. Phosphoinositide signaling pathways in nuclei are associated with nuclear speckles containing pre-mRNA processing factors. Mol Biol Cell. 1998; 9:3547–3560. [PubMed: 9843587]
15. Silacci P, Mazzolai L, Gauci C, Stergiopulos N, Yin HL, Hayoz D. Gelsolin superfamily proteins: key regulators of cellular functions. Cell Mol Life Sci. 2004; 61:2614–2623. [PubMed: 15526166]
16. Yonezawa N, Nishida E, Iida K, Yahara I, Sakai H. Inhibition of the interactions of cofilin, destrin, and deoxyribonuclease I with actin by phosphoinositides. J Biol Chem. 1990; 265:8382–8386. [PubMed: 2160454]
17. Yamamoto M, Hilgemann DH, Feng S, Bito H, Ishihara H, Shibasaki Y, Yin HL. Phosphatidylinositol 4,5-bisphosphate induces actin stress-fiber formation and inhibits membrane ruffling in CV1 cells. J Cell Biol. 2001; 152:867–876. [PubMed: 11238445]
18. Raucher D, Stauffer T, Chen W, Shen K, Guo S, York JD, Sheetz MP, Meyer T. Phosphatidylinositol 4,5-bisphosphate functions as a second messenger that regulates cytoskeleton-plasma membrane adhesion. Cell. 2000; 100:221–228. [PubMed: 10660045]

19. Mejillano M, Yamamoto M, Rozelle AL, Sun HQ, Wang X, Yin HL. Regulation of apoptosis by phosphatidylinositol 4,5-bisphosphate inhibition of caspases, and caspase inactivation of phosphatidylinositol phosphate 5-kinases. J Biol Chem. 2001; 276:1865–1872. [PubMed: 11042212]
20. Azuma T, Koths K, Flanagan L, Kwiatkowski D. Gelsolin in complex with phosphatidylinositol 4,5-bisphosphate inhibits caspase-3 and -9 to retard apoptotic progression. J Biol Chem. 2000; 275:3761–3766. [PubMed: 10660524]
21. Halstead JR, van Rheenen J, Snel MH, Meeuws S, Mohammed S, D'Santos CS, Heck AJ, Jalink K, Divecha N. A role for PtdIns(4,5)P2 and PIP5Kalpha in regulating stress-induced apoptosis. Curr Biol. 2006; 16:1850–1856. [PubMed: 16979564]
22. Holz RW, Hlubek MD, Sorensen SD, Fisher SK, Balla T, Ozaki S, Prestwich GD, Stuenkel EL, Bittner MA. A pleckstrin homology domain specific for phosphatidylinositol 4, 5-bisphosphate (PtdIns-4,5-P2) and fused to green fluorescent protein identifies plasma membrane PtdIns-4,5-P2 as being important in exocytosis. J Biol Chem. 2000; 275:17878–17885. [PubMed: 10747966]
23. Aikawa Y, Martin TF. ARF6 regulates a plasma membrane pool of phosphatidylinositol(4,5)bisphosphate required for regulated exocytosis. J Cell Biol. 2003; 162:647–659. [PubMed: 12925709]
24. Milosevic I, Sorensen JB, Lang T, Krauss M, Nagy G, Haucke V, Jahn R, Neher E. Plasmalemmal phosphatidylinositol-4,5-bisphosphate level regulates the releasable vesicle pool size in chromaffin cells. J Neurosci. 2005; 25:2557–2565. [PubMed: 15758165]
25. James DJ, Khodthong C, Kowalchyk JA, Martin TF. Phosphatidylinositol 4,5-bisphosphate regulates SNARE-dependent membrane fusion. J Cell Biol. 2008; 182:355–366. [PubMed: 18644890]
26. Waselle L, Gerona RR, Vitale N, Martin TF, Bader MF, Regazzi R. Role of phosphoinositide signaling in the control of insulin exocytosis. Mol Endocrinol. 2005; 19:3097–3106. [PubMed: 16081518]
27. Zhang J, Luo R, Wu H, Wei S, Han W, Li G. Role of type I{alpha} phosphatidylinositol-4-phosphate 5-kinase in insulin secretion, glucose metabolism, and membrane potential in INS-1 {beta}-cells. Endocrinology. 2009; 150:2127–35. [PubMed: 19116346]
28. Di Paolo G, De Camilli P. Phosphoinositides in cell regulation and membrane dynamics. Nature. 2006; 443:651–657. [PubMed: 17035995]
29. Cremona O, Di Paolo G, Wenk MR, Luthi A, Kim WT, Takei K, Daniell L, Nemoto Y, Shears SB, Flavell RA, McCormick DA, De Camilli P. Essential role of phosphoinositide metabolism in synaptic vesicle recycling. Cell. 1999; 99:179–188. [PubMed: 10535736]
30. Tsuboi T, McMahon HT, Rutter GA. Mechanisms of dense core vesicle recapture following “kiss and run” (“cavicapture”) exocytosis in insulin-secreting cells. J Biol Chem. 2004; 279:47115–47124. [PubMed: 15331588]
31. Varnai P, Balla T. Visualization of phosphoinositides that bind pleckstrin homology domains: calcium-and agonist-induced dynamic changes and relationship to myo-[3H]inositol-labeled phosphoinositide pools. J Cell Biol. 1998; 143:501–510. [PubMed: 9786958]
32. Tomas A, Yermen B, Min L, Pessin JE, Halban PA. Regulation of pancreatic beta-cell insulin secretion by actin cytoskeleton remodelling: role of gelsolin and cooperation with the MAPK signalling pathway. J Cell Sci. 2006; 119:2156–2167. [PubMed: 16638805]
33. Tomas A, Meda P, Regazzi R, Pessin JE, Halban PA. Munc 18-1 and granuphilin collaborate during insulin granule exocytosis. Traffic. 2008; 9:813–832. [PubMed: 18208509]
34. Yermen B, Tomas A, Halban PA. Pro-survival role of gelsolin in mouse beta-cells. Diabetes. 2007; 56:80–87. [PubMed: 17192468]
35. Naslavsky N, Weigert R, Donaldson JG. Convergence of non-clathrin- and clathrin-derived endosomes involves Arf6 inactivation and changes in phosphoinositides. Mol Biol Cell. 2003; 14:417–431. [PubMed: 12589044]
36. Pouli AE, Emmanouilidou E, Zhao C, Wasmeier C, Hutton JC, Rutter GA. Secretory-granule dynamics visualized in vivo with a phogrin-green fluorescent protein chimaera. Biochem J. 1998; 333:193–199. [PubMed: 9639579]

37. Tsuboi T, Rutter GA. Multiple forms of “kiss-and-run” exocytosis revealed by evanescent wave microscopy. Curr Biol. 2003; 13:563–567. [PubMed: 12676086]
38. Nagai T, Ibata K, Park ES, Kubota M, Mikoshiba K, Miyawaki A. A variant of yellow fluorescent protein with fast and efficient maturation for cell-biological applications. Nat Biotechnol. 2002; 20:87–90. [PubMed: 11753368]
39. Sun HQ, Yamamoto M, Mejillano M, Yin HL. Gelsolin, a multifunctional actin regulatory protein. J Biol Chem. 1999; 274:33179–33182. [PubMed: 10559185]
40. Ridley AJ. Rho GTPases and actin dynamics in membrane protrusions and vesicle trafficking. Trends Cell Biol. 2006; 16:522–529. [PubMed: 16949823]
41. Yamazaki M, Miyazaki H, Watanabe H, Sasaki T, Maehama T, Frohman MA, Kanaho Y. Phosphatidylinositol 4-phosphate 5-kinase is essential for ROCK-mediated neurite remodeling. J Biol Chem. 2002; 277:17226–17230. [PubMed: 11877391]
42. Hammar E, Tomas A, Bosco D, Halban PA. Role of the Rho-Rock (Rho-associated kinase) signaling pathway in the regulation of pancreatic beta cell function. Endocrinology. 2009; 150:2072–9. [PubMed: 19106222]
43. Frantz C, Coppola T, Regazzi R. Involvement of Rho GTPases and their effectors in the secretory process of PC12 cells. Exp Cell Res. 2002; 273:119–126. [PubMed: 11822867]
44. Hay JC, Fisette PL, Jenkins GH, Fukami K, Takenawa T, Anderson RA, Martin TF. ATP-dependent inositide phosphorylation required for Ca(2+)-activated secretion. Nature. 1995; 374:173–177. [PubMed: 7877690]
45. Gong LW, Di Paolo G, Diaz E, Cestra G, Diaz ME, Lindau M, De Camilli P, Toomre D. Phosphatidylinositol phosphate kinase type I gamma regulates dynamics of large dense-core vesicle fusion. Proc Natl Acad Sci U S A. 2005; 102:5204–5209. [PubMed: 15793002]
46. Begle A, Tryoen-Toth P, de Barry J, Bader MF, Vitale N. ARF6 regulates the synthesis of fusogenic lipids for calcium-regulated exocytosis in neuroendocrine cells. J Biol Chem. 2009; 284:4836–45. [PubMed: 19124467]
47. Aoyagi K, Sugaya T, Umeda M, Yamamoto S, Terakawa S, Takahashi M. The activation of exocytotic sites by the formation of phosphatidylinositol 4,5-bisphosphate microdomains at syntaxin clusters. J Biol Chem. 2005; 280:17346–17352. [PubMed: 15741173]
48. Olsen HL, Hoy M, Zhang W, Bertorello AM, Bokvist K, Capito K, Efanov AM, Meister B, Thams P, Yang SN, Rorsman P, Berggren PO, Gromada J. Phosphatidylinositol 4-kinase serves as a metabolic sensor and regulates priming of secretory granules in pancreatic beta cells. Proc Natl Acad Sci U S A. 2003; 100:5187–5192. [PubMed: 12700357]
49. Galiano FJ, Ulug ET, Davis JN. Overexpression of murine phosphatidylinositol 4-phosphate 5-kinase type Ibeta disrupts a phosphatidylinositol 4,5 bisphosphate regulated endosomal pathway. J Cell Biochem. 2002; 85:131–145. [PubMed: 11891857]
50. Kanzaki M, Furukawa M, Raab W, Pessin JE. Phosphatidylinositol 4,5-bisphosphate regulates adipocyte actin dynamics and GLUT4 vesicle recycling. J Biol Chem. 2004; 279:30622–30633. [PubMed: 15123724]
51. Cremona O, De Camilli P. Phosphoinositides in membrane traffic at the synapse. J Cell Sci. 2001; 114:1041–1052. [PubMed: 11228149]
52. Krauss M, Kinuta M, Wenk MR, De Camilli P, Takei K, Haucke V. ARF6 stimulates clathrin/AP-2 recruitment to synaptic membranes by activating phosphatidylinositol phosphate kinase type Igamma. J Cell Biol. 2003; 162:113–124. [PubMed: 12847086]
53. Lawrence JT, Birnbaum MJ. ADP-ribosylation factor 6 regulates insulin secretion through plasma membrane phosphatidylinositol 4,5-bisphosphate. Proc Natl Acad Sci U S A. 2003; 100:13320–13325. [PubMed: 14585928]
54. Coppola T, Hirling H, Perret-Menoud V, Gattesco S, Catsicas S, Joberty G, Macara IG, Regazzi R. Rabphilin dissociated from Rab3 promotes endocytosis through interaction with Rabaptin-5. J Cell Sci. 2001; 114:1757–1764. [PubMed: 11309205]
55. Vo YP, Hutton JC, Angleson JK. Recycling of the dense-core vesicle membrane protein phogrin in Min6 beta-cells. Biochem Biophys Res Commun. 2004; 324:1004–1010. [PubMed: 15485654]

56. Kimura T, Kaneko Y, Yamada S, Ishihara H, Senda T, Iwamatsu A, Niki I. The GDP-dependent Rab27a effector coronin 3 controls endocytosis of secretory membrane in insulin-secreting cell lines. J Cell Sci. 2008; 121:3092–3098. [PubMed: 18768935]
57. Min L, Leung YM, Tomas A, Watson RT, Gaisano HY, Halban PA, Pessin JE, Hou JC. Dynamin is functionally coupled to insulin granule exocytosis. J Biol Chem. 2007; 282:33530–33536. [PubMed: 17848579]
58. Sechi AS, Wehland J. The actin cytoskeleton and plasma membrane connection: PtdIns(4,5)P(2) influences cytoskeletal protein activity at the plasma membrane. J Cell Sci. 2000; 113:3685–3695. [PubMed: 11034897]
59. Lilla V, Webb G, Rickenbach K, Maturana A, Steiner DF, Halban PA, Irminger JC. Differential gene expression in well-regulated and dysregulated pancreatic beta-cell (MIN6) sublines. Endocrinology. 2003; 144:1368–1379. [PubMed: 12639920]
60. Bosco D, Meda P, Halban PA, Rouiller DG. Importance of cell-matrix interactions in rat islet beta-cell secretion in vitro: role of alpha6beta1 integrin. Diabetes. 2000; 49:233–243. [PubMed: 10868940]
61. Holz RW, Brondyk WH, Senter RA, Kuizon L, Macara IG. Evidence for the involvement of Rab3A in Ca(2+)-dependent exocytosis from adrenal chromaffin cells. J Biol Chem. 1994; 269:10229–10234. [PubMed: 8144603]
62. Gavrieli Y, Sherman Y, Ben-Sasson SA. Identification of programmed cell death in situ via specific labeling of nuclear DNA fragmentation. J Cell Biol. 1992; 119:493–501. [PubMed: 1400587]

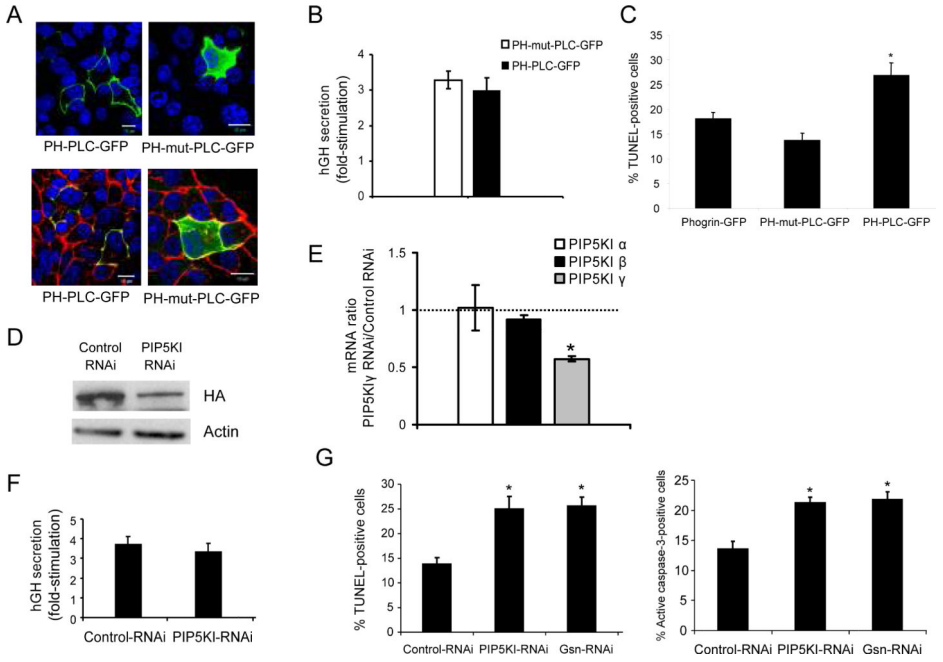

Figure 1. Effects of decreasing levels of PIP_2 on beta cell survival and insulin secretion

(A) Immunofluorescence analysis of MIN6B1 cells transfected with the PIP_2 blocking vector PH-PLCGFP (lefts panels) or PH-mut-PLC-GFP as a control (right panels). GFP vectors are depicted in green; F-actin, red (bottom panels); DNA, blue. Bars, 10 μM. (B) Fold-stimulation of hGH secretion (glucose-stimulated/basal secretion) from MIN6B1 cells cotransfected with PH-mut-PLC-GFP or PH-PLC-GFP and an hGH-coding vector (used as a surrogate marker for secretion from transfected cells only). N=9 from 3 independent experiments. (C) MIN6B1 cells were transfected with phogrin-GFP (control), PH-mut-PLC or PH-PLC-GFP and apoptosis of GFP-positive cells was measured by TUNEL after 48 h incubation in deprived conditions. N=4; *p<0.02 vs. phogrin-GFP. (D) Knock-down of PIP5KIγ by RNAi: MIN6B1 cells were co-transfected with HAPIP5KI and either pSUPER-Control RNAi or pSUPER-PIP5KI RNAi. After 72 h, expression of HA-tagged PIP5KIγ and actin (loading control) was examined by Western blot. (E) Quantitative RT-PCR results showing relative mRNA levels for the 3 mouse PIP5KI isoforms (α, β and γ) in pSUPERPIP5KIγ RNAi over pSUPER-Control RNAitransfected cells. N=4 from 2 independent experiments, *$p<2{\cdot}10^{-6}$. (F) Fold-stimulation in hGH secretion of MIN6B1 cells co-transfected with pSUPER-Control RNAi or pSUPER-PIP5KI RNAi and hGH. N=9 from 3 independent experiments. (G) Apoptosis of GFP-positive MIN6 B1 cells was measured in deprived conditions by TUNEL (left graph) or active-caspase 3 (right graph) in cells cotransfected with phogrin-GFP and either pSUPER-Control RNAi, pSUPER-PIP5KI RNAi or pSUPERGsn RNAi plasmids. N=4, *p<0.04 vs. control RNAi.

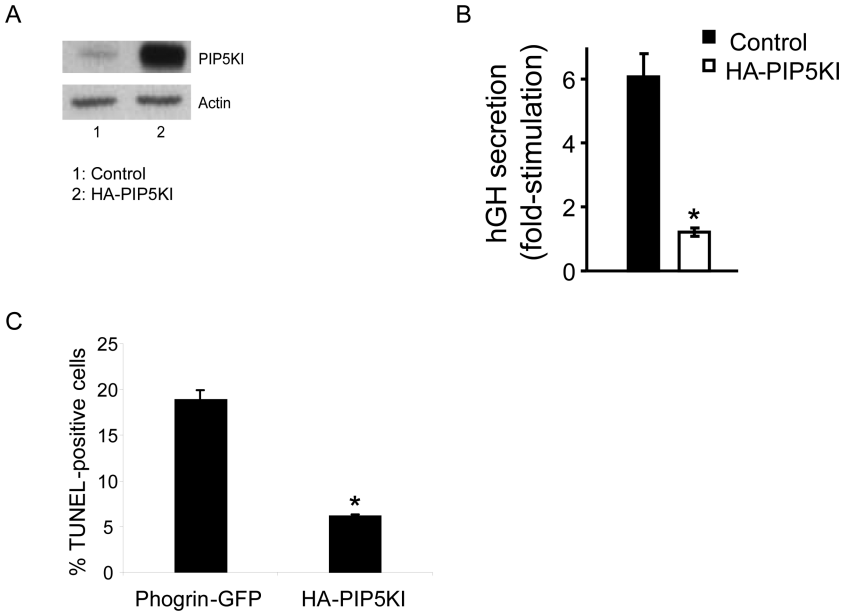

Figure 2. Over-expression of PIP5KIγ protects beta cells from apoptosis but disturbs normal secretory response to glucose

(A) Western blot analysis of the level of PIP5KIγ and actin (loading control) in MIN6B1 cells transfected with HA-PIP5KI (lane 2) vs. control empty plasmid (Lane 1). (B) Fold-stimulation of hGH secretion from MIN6B1 cells co-transfected with control empty vector or HAPIP5KI and hGH. N=9 from 3 independent experiments, *$p<5{\cdot}10^{-6}$. (C) Percentage of apoptotic MIN6B1 cells after transfection with phogrin-GFP (control) or HA-PIP5KI. Apoptosis specifically from GFP- or HA-positive cells was measured in deprived conditions by TUNEL. N=3, *$p<0.001$.

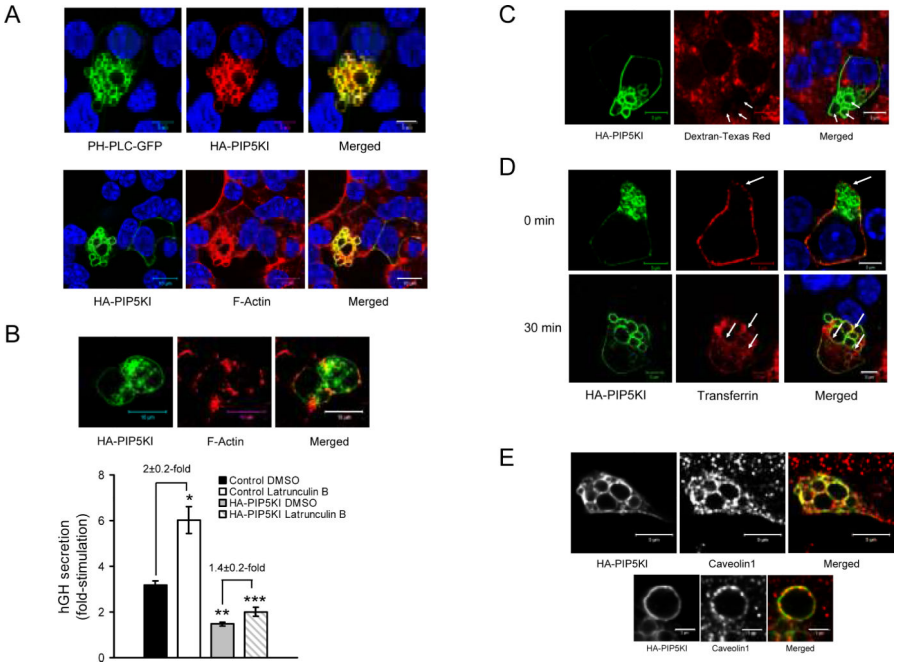

Figure 3. Over-expression of PIP5KIγ results in the accumulation of PIP_2-positive endocytic vacuoles in the cytoplasm of MIN6B1 cells

(A, top) Immunofluorescence of MIN6B1 cells cotransfected with PH-PLC-GFP (green) and HAPIP5KI (red). (A, bottom) Immunofluorescence of cells transfected with HA-PIP5KI showing the vacuoles coated with F-actin. HA-PIP5KI (detected with an anti-HA tag antibody), green; F-actin, red; DNA, blue. (B, top) F-actin depolymerization affects vacuole morphology but not vacuole formation: HAPIP5KI-transfected MIN6B1 cells were treated with latrunculin B for 2 hours prior to fixation. HA-PIP5KI vacuoles are still present (green) even though F-actin is extensively depolymerized and the vacuoles are no longer actin-coated (red). (B, bottom) Fold-stimulation of hGH secretion from MIN6B1 cells cotransfected with hGH and either an empty vector or HA-PIP5KI and pre-treated for 2 hours with DMSO (control) or latrunculin B. N=9 from 3 independent experiments (*$p<6{\cdot}10^{-4}$ and **$p<10^{-6}$ vs. control DMSO; ***$p<0.03$ vs. HA-PIP5KI DMSO). (C) Fluid-phase uptake assay performed in HA-PIP5KI-transfected MIN6B1 cells by incubation for 30 min with lysine-fixable Texas Red-dextran prior to fixation. HA-PIP5KI is depicted in green; Texas Red-dextran, red; DNA, blue. (D) TfR internalization assay in vacuole-containing HA-PIP5KI-transfected MIN6B1 cells co-transfected with a plasmid encoding human TfR shows that the vacuole membrane has a clathrin-dependent endocytic origin. HA-PIP5KI is in green; AlexaFluor 555-human transferrin, red; DNA, blue. (E) Clathrin-independent endocytic membrane also accumulates at PIP5KIγ-induced vacuoles: MIN6B1 cells were transfected with HA-PIP5KI, fixed and labeled by immunofluorescence for caveolin 1. Note how caveolin 1-positive staining is apparent at the vacuolar membrane (top, and in a zoomed-in vacuole, bottom). HA-PIP5KI, green; caveolin 1, red in the merged panel.

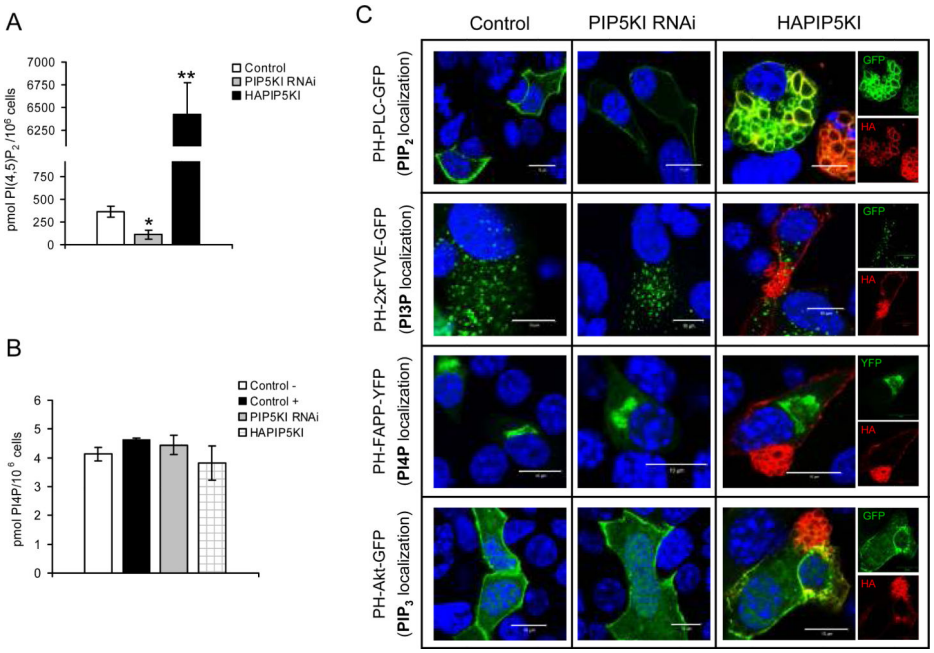

Figure 4. Quantification and subcellular localization of phosphoinositides in MIN6 B1 cells after PIP5KIγ over-expression and knock-down by RNAi

(A) PIP_2 level measured in control untransfected cells and in cells transfected with either pSUPER-PIP5KI RNAi or HA-PIP5KI. Data has been corrected according to the estimated transfection efficiency for each plasmid (~70% for pSUPER-PIP5KI RNAi and ~15% for HA-PIP5KI). N=3-5, *$p<0.04$ and **$p<5\cdot10^{-7}$ vs. control. (B) The level of PI4P was determined in untransfected cells (control −), and in cells transfected with either an empty vector (control +), HA-PIP5KI or pSUPERPIP5KI RNAi. N=2. (C) Immunofluorescence analysis of MIN6B1 cells co-transfected with a control empty vector (left panels), pSUPER-PIP5KI RNAi (central panels) or HA-PIP5KI (right panels; merged, green and red images) and a series of constructs expressing specific phosphoinositide-recognition domains fused to GFP or YFP (depicted in green): PH-PLC-GFP (for PIP_2 localization), PH-2xFYVE-GFP (for PI3P localization), PH-FAPP-YFP (for PI4P localization), and PH-Akt-GFP (for PIP_3 localization). HA-PIP5KI (detected with an anti-HA tag antibody), red; DNA, blue.

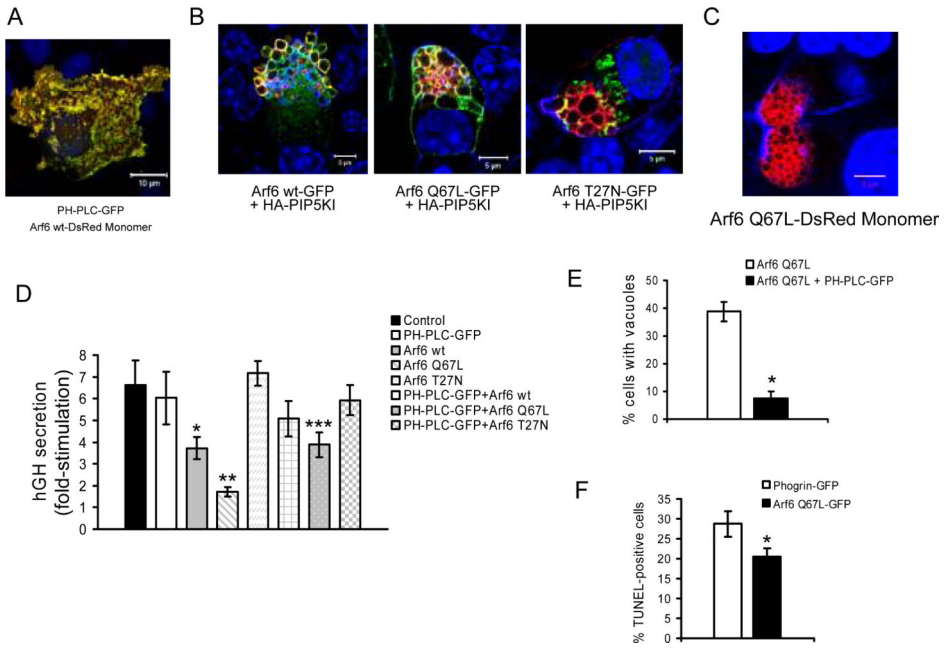

Figure 5. Arf6-dependent activation of PIP5KIγ results in impaired insulin secretion and blockage of the endocytic pathway in MIN6B1 cells

(A) MIN6B1 cells were co-transfected with PH-PLC-GFP and Arf6 wt-DsRed Monomer and basal membranes were observed by confocal microscopy. PH-PLC-GFP, green; Arf6 wt-DsRed Monomer, red; DNA, blue. (B) MIN6B1 cells were co-transfected with HA-PIP5KI and either Arf6 wt-GFP, Arf6 Q67L-GFP or Arf6 T27N-GFP prior to fixation. HA-PIP5KI, red; GFP fusion constructs, green; DNA, blue. (C) MIN6B1 cells expressing Arf6 Q67L-DsRed Monomer accumulate similar vacuoles to HA-PIP5KI-expressing cells. Arf6 Q67L-DsRed Monomer, red; F-actin and DNA, blue. (D) Fold-stimulation of hGH secretion from MIN6B1 cells cotransfected with hGH and a series of constructs including: control empty vector, PH-PLC-GFP, Arf6 wt-HA, Arf6 Q67L-HA, Arf6 T27N-HA, and a combination of PH-PLC-GFP and Arf6 wt-HA, Arf6 Q67L-HA or Arf6 T27N-HA (estimated level of cotransfection ≥95%). N=18 from 6 independent experiments (*$p<0.03$ and **$p<0.0006$ vs. control; ***$p<0.003$ vs. Arf6 Q67L-HA). (E) Percentage of vacuole-containing cells after transfection with Arf6 Q67L-DsRed Monomer alone or in combination with PH-PLC-GFP. *$p<2{\cdot}10^{-6}$. (F) Percentage of apoptotic MIN6B1 cells after transfection with phogrin-GFP (control) or Arf6 Q67L-GFP, measured specifically from GFP- positive cells in deprived conditions by TUNEL. N=4, *$p<0.04$.

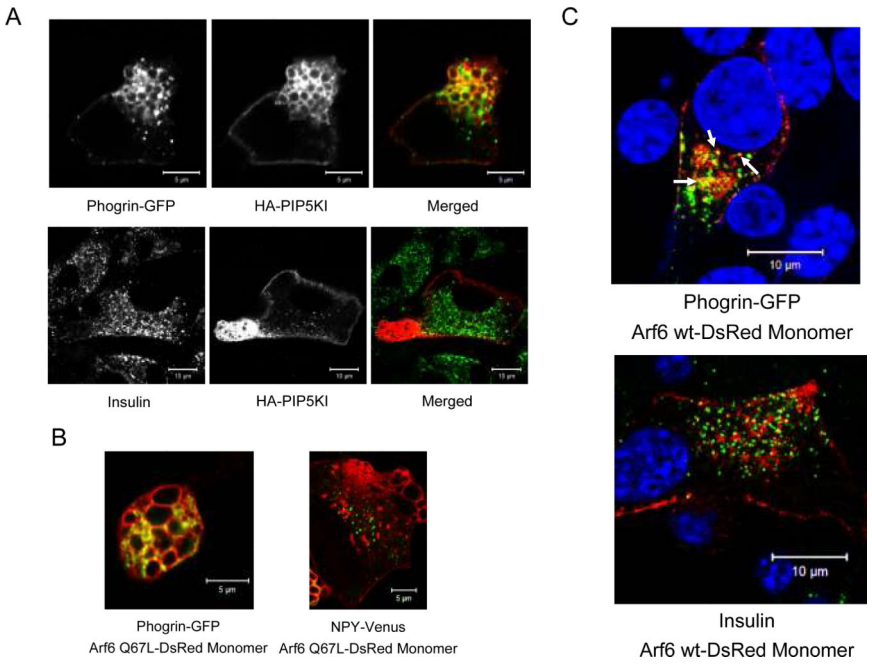

Figure 6. Endocytic vacuoles accumulated in the cytoplasm of MIN6B1 cells after PIP5KIγ over-expression or Arf6 over-activation contain the granular membrane protein phogrin but are devoid of insulin

(A) MIN6B1 cells were cotransfected with HA-PIP5KI and phogrin-GFP. Phogrin was detected in granules and at the membrane of the vacuoles in PIP5KI-over-expressing cells (top panels), while insulin (granule cargo) was present in granules but absent from vacuoles (bottom panels). Phogrin-GFP is in green and HA-PIP5KI, red in the merged top panel; insulin, green and HA-PIP5KI, red in the merged bottom panel. (B) MIN6B1 cells were co-transfected with Arf6 Q67L-DsRed Monomer and either phogrin-GFP or NPY-Venus (as a surrogate marker for granule cargo in living cells), and analyzed by confocal live microscopy. As for HA-PIP5KI vacuoles, phogrin-GFP (green) is detected at the membrane of (red) Arf6-positive vacuoles (left panel), while NPY-Venus (green) is excluded from the vacuolar interior (right panel). (C) MIN6B1 cells were co-transfected with Arf6 wt-DsRed Monomer and phogrin-GFP. Note some examples of cytoplasmic phogrin-GFP granules (green) also positive for Arf6 (red) (top panel, arrows) while insulin (green) does not co-localize with Arf6 (red) (bottom panel).

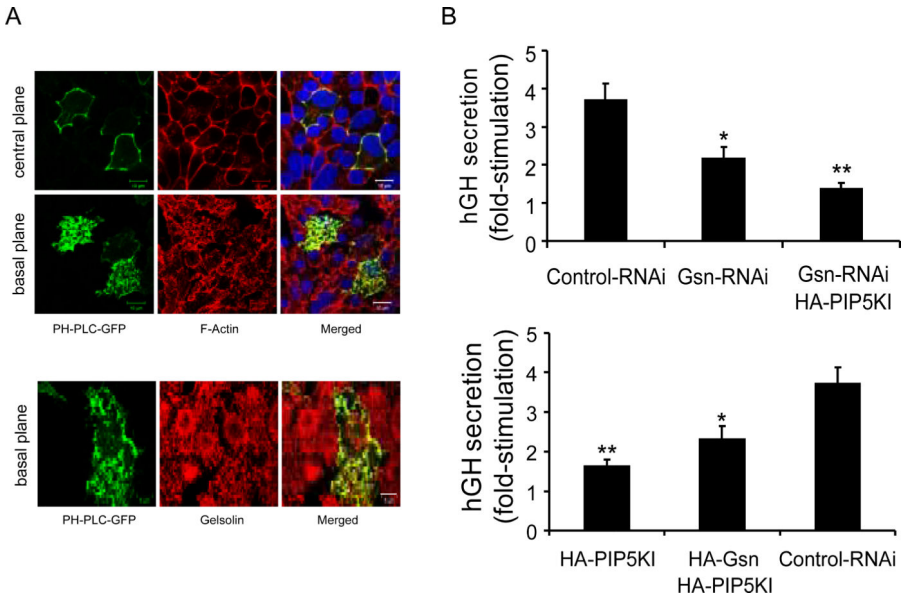

Figure 7. Inhibition of the actin-remodeling protein gelsolin in cells with increased level of PIP_2 contributes to the reduction of glucose-stimulated insulin secretion

(A) Immunofluorescence analysis of PH-PLC-GFP-transfected MIN6B1 cells. PH-PLC-GFP, green; F-actin (top panels) and gelsolin (bottom panels), red; DNA, blue. (B) Fold-stimulation of hGH secretion from MIN6B1 cells co-transfected with hGH and pSUPER-Control RNAi, pSUPER-Gsn RNAi, or a combination of pSUPER-Gsn RNAi and HA-PIP5KI (top graph); or pSUPER-Control RNAi, HA-PIP5KI or a combination of HA-Gsn and HA-PIP5KI (bottom graph). N=15 from 5 independent experiments (top graph: *p<0.004 vs. control; **p<0.01 vs. pSUPERGsn RNAi; bottom graph: *p<0.04 vs. HA-PIP5KI; **p<$5\cdot10^{-5}$ vs. control).

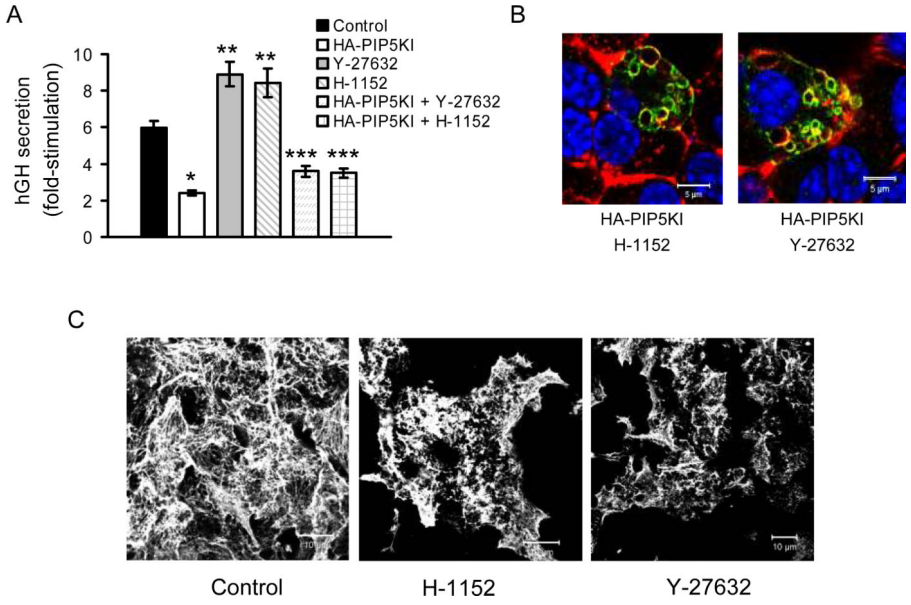

Figure 8. The Rho-ROCK pathway is implicated in the reduction of glucose-stimulated insulin secretion due to over-activation of PIP5KIγ via a different mechanism than the Arf6 pathway

(A) Fold-stimulation of hGH secretion from MIN6B1 cells co-transfected with hGH and either a control empty vector or the HA-PIP5KI plasmid and pre-treated for 2 h with or without ROCK inhibitors Y-2 7 6 3 2 o r H-1152. N=9 from 3 independent experiments (*$p<4{\cdot}10^{-7}$ and **$p<0.02$ vs. control; ***$p<3{\cdot}10^{-5}$ vs. Y-27632 or H-1152 alone). (B) Cells were transfected with HA-PIP5KI and treated for 2 h with Y-27632 or H-1152 prior to fixation. HA-PIP5KI, green; F-actin, red; DNA, blue. (C) MIN6B1 cells were left untreated or incubated with Y-27632 or H-1152 for 2 h before fixation and confocal microscopy analysis. The F-actin fibers (stained with fluorescent phalloidin) are shorter in the cytoskeleton of MIN6B1 cells after treatment with ROCK inhibitors compared to the control.

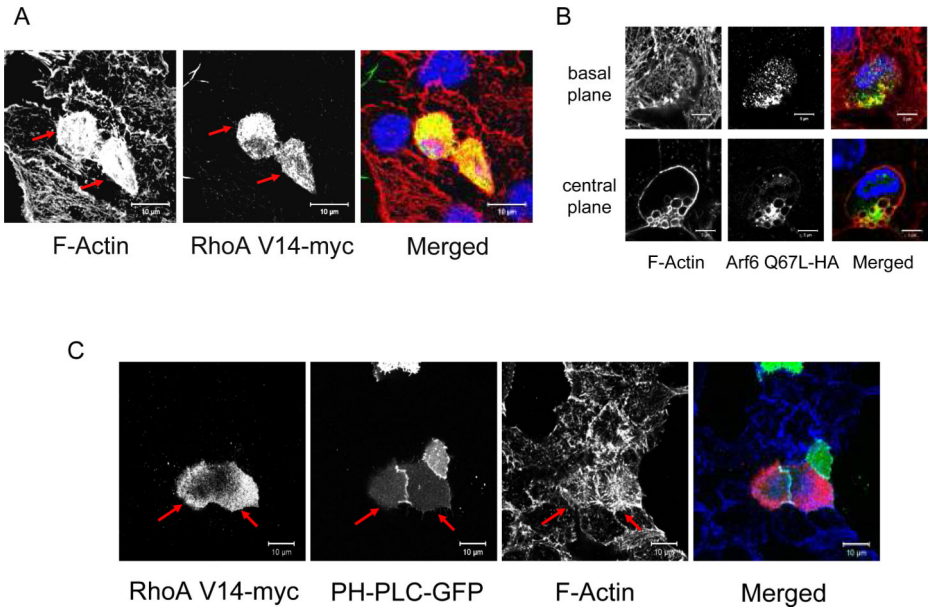

Figure 9. Over-activation of the Rho-ROCK pathway results in disturbance of actin cytoskeleton remodeling in MIN6B1 cells which is partially counteracted by PIP_2 blockage

(A) MIN6B1 cells were transfected with RhoA V14-myc, fixed and analyzed by immunofluorescence. Note how the F-actin cytoskeleton forms a denser mesh of fibers in cells expressing RhoA V14-myc (red arrows) than in control untransfected cells from the same dish. F-actin, red; RhoA V14-myc (detected with an anti-myc tag antibody), green; DNA, blue in the merged panel. (B) MIN6B1 cells were transfected with Arf6 Q67L-HA. The same cell is depicted at the basal membrane (upper panels) and at the cell centre (lower panels). Note how the F-actin cytoskeleton is unchanged in cells expressing Arf6 Q67L-HA compared to control untransfected neighboring cells, apart from the accumulation of F-actin-coated Arf6-positive vacuoles. F-actin, red; Arf6 Q67L-HA (detected with an anti-HA tag antibody), green; DNA, blue in the merged panel. (C) MIN6B1 cells were co-transfected with RhoA V14-myc and PH-PLC-GFP. Note how cells expressing both constructs (red arrows) display a less dense actin cytoskeleton than cells transfected with RhoA V14-myc alone (compare to Figure 8A), resembling that of neighboring untransfected cells from the same dish. PH-PLC-GFP, green; RhoA V14-myc, red; F-actin, blue in the merged panel.